

# Parametric Investigation On The Behaviour Of Concrete Filled Tell Tubes

A. Singh<sup>1</sup>, S. Kumar<sup>2</sup>, U. Mani<sup>3</sup> and A. Tripathi<sup>4</sup>

<sup>1</sup> Department of Civil Engineering, Rama University, Kanpur, India

<sup>2</sup> Department of Civil Engineering, Rama University, Kanpur, India

<sup>3</sup> Department of Civil Engineering, Rama University, Kanpur, India

<sup>4</sup> Department of Civil Engineering, Rama University, Kanpur, India

**Abstract:** The use of concrete-filled steel tubes (CFST) in engineering structures has become popular because of their excellent seismic resistance structural properties such as high strength, high ductility and large energy absorption capacity. In CFSTs the surrounding steel tube provides effective confinement to the filled-in concrete and in turn the concrete helps to reduce the potential local buckling of the steel tube resulting improved seismic resistant performance. Concrete filled steel tube (CFST) columns are widely used in civil engineering structures due to its abundant structural benefits like excellent seismic behavior, ultimate load bearing capacity, fire resistivity, excellent ductility and energy absorption capacity, particularly in zones of high seismic risk. Due to their excellent engineering properties, CFST columns are used in buildings, bridges, electric transmission line and offshore structures. The ultimate load carrying capacity of CFST columns depends upon various parameters such as D/t ratio, steel grade, concrete grade, etc. Abaqus software is used for the finite element modelling of CFST Columns. In this study the ultimate axial load carrying capacity of CFST column is investigated by changing diameter-to thickness (D/t) ratio, steel grade and concrete grade. Results shows that the ultimate load capacity decreases by increase in D/t ratio but increases by increase in steel grade and concrete grade. Behaviour of composite steel-concrete elements in various loading stages is quite well analysed by theoretical investigations and experiments. Concrete-Filled Steel Tube (CFST) is one of many composite elements used at present in civil engineering. Different approaches and design philosophies were adopted in different design codes for it. But for hollow CFST elements, which are more effective than ordinary CFST, any code does not provide information about how to design these elements. Further investigations of hollow composite CFST elements are needed. In loading stage, when a particular level of stresses exists, an interaction between steel tube and concrete core appears and therefore a complex stress state of element takes place, which increases the load-bearing capacity of the whole composite element. This interaction between components of CFST elements is reached because of different material properties, such as Poisson's ratio, elasticity modulus etc. In this article reasons of the above-mentioned complex stress state appearance and behaviour of hollow CFST element components in different load stages of compressed stub structural member are analysed. The test results are presented in diagrams, tables. Previous researches of other investigators are summarised. Differences and similarities in behaviour of solid concrete and composite elements and hollow members with different number of concrete core layers are discussed.

**Keywords:** Drunken Pecker Model; Plastic failure; material non-linearity; finite element method; Fin plate connection; Micro-cracking

## I. INTRODUCTION

Concrete-filled steel tubular (CFST) columns are becoming widely used in the construction of building structures, especially high-rise buildings. Their attractive features include greater load-bearing capacity and fire resistance of CFSTs compared to traditional steel or concrete columns with the same size, enhancement of material performance in composite action compared to steel or concrete acting alone. CFST columns are favoured by architects owing to their slender and attractive appearance (Ding and Wang, 2008). A fundamental assumption in using CFST columns is that the steel tube and the infilled concrete are both engaged in composite action to resist the applied external load. Many experimental and numerical research studies have been conducted on the structural behaviour and fire resistance of concrete-filled steel tubular columns. However, these studies have mainly been focused on isolated CFST

columns where the external loads are directly applied on top. In realistic structures, in contrast, part of the load on a column is applied by the connected beams through connections. The process of applying the load to a CFST column through the connection is commonly defined as “load introduction”. In a column made of one material such as steel or concrete, the applied load on the connected beam is easily transferred. However, a CFST column is made of two materials, a steel tube and a concrete core. Furthermore, connections are commonly attached to the external steel tube surface, such as when using the common fin plate connection as shown in fig below, for ease of construction.

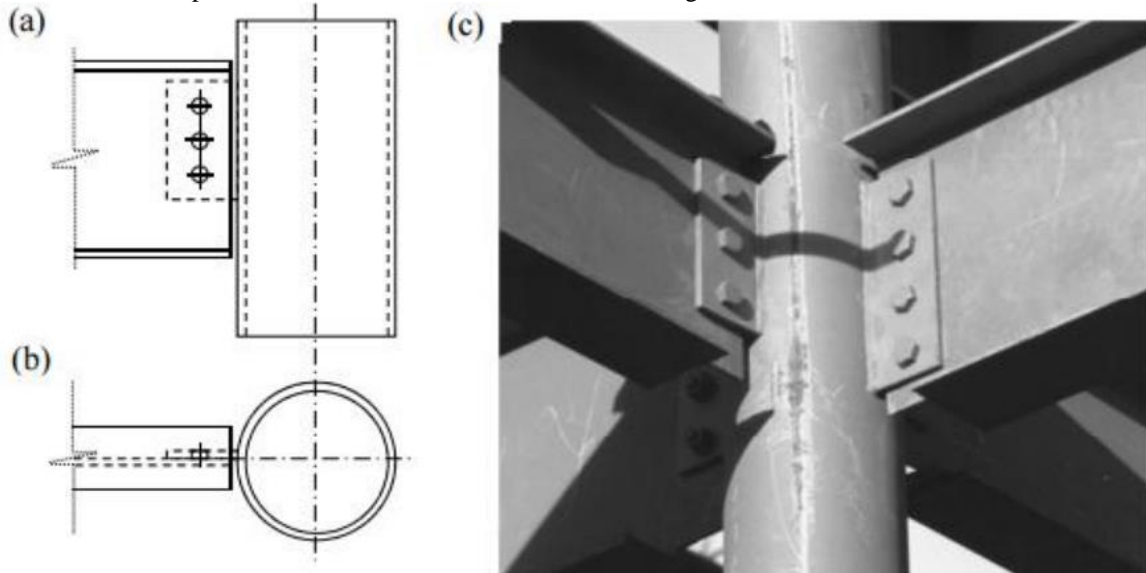


Fig.1 Single shear fin plate connection to circular hollow section view (a) Elevation view (b) Section view (c) 3D view of actual construction .

As a result, since the load to be introduced to the CFST column is not applied directly to the entire column, the applied load is gradually transferred from the steel tube to the concrete core. In the current design approaches, such as Eurocode 4 (CEN, 2004) and AISC Specification (AISC, 2010), load introduction is assumed to occur through the steel tube/concrete core bond within an “introduction length”. The introduction length according to Eurocode 4 (CEN, 2004) is assumed to be a minimum of  $2D$  or  $L/3$  if less, where  $D$  is the minimum dimension of the column cross-section and  $L$  is the length of the column. In Eurocode 4 (CEN, 2004), the load introduction region is not explicitly specified, but is believed to be below the connection. In the AISC Specification (AISC, 2010), the load introduction length is limited to  $2D$  both above and below the connection. If the bond loading capacity within the load introduction length is not sufficient, which is usually the case, Eurocode 4 (CEN, 2004) suggests placing shear connectors inside the steel tube to help transfer the introduced load from the steel tube to the concrete core. However, this method is highly uneconomical and impractical since accessibility to the inside of the steel tube for installation of shear connectors is very difficult, especially for the tubes with smaller diameters. Furthermore, because the slip between the steel and the concrete may not be big enough to enable the shear connectors to develop their design strength, the effectiveness of the shear connectors is questionable (MacRae et al., 2004). As an alternative, Kurobane et al. (2004) suggest using a through-plate connection

However, this type of connection can be time-consuming to construct, and also it would be feasible in only one direction as the through-plate in the other direction would be blocked. Under fire condition, due to loss of bond between the steel tube and the concrete core in the heated CFST member, the implied load introduction mechanism disappears. Through-plate connection becomes the only possible solution, as recommended by Kodur and MacKinnon (2000).

If the internal shear connectors are to be dispensed with, a possible design approach for CFST columns with insufficient bond loading capacity is to allow partial transfer of the introduced load to the concrete core. The CIDECT design guide (Kurobane et al., 2004) recommends decreasing the concrete design strength, based on the experimental results of Dunberry et al. (1987). However, there is a fundamental mistake in the assumed load introduction mechanism. Figure 1.3 shows a free body diagram in a CFST column just below the connection (section A-A). As can be seen, the total force in the CFST column remains constant throughout the column length underneath the connections until the bottom of the column. Therefore, for the column to achieve plastic resistance of the cross-section, the resistance must be achieved just underneath the

connections. This means that load transfer below the connections is the process of reducing the force in the steel tube and increasing the force in the concrete core, but without any increase in the resistance of the Section. Therefore, any construction detailed below the connection, such as using shear connectors inside the steel tube, would not have the intended effect of the total resistance of the CFST column.

The existing design guides can all be traced back to the experiments of Dunberry et al. (1987). However, as will be in detail explained in section 2.4.2, this research only tested a small number of arrangements. Many of these tests do not reflect realistic construction conditions. More critically, the most important tests, examining partial load introduction, did not yield useful results due to experimental failure. Therefore, a complete reinvestigation is necessary. This new research should not only seek to understand the correct mechanism of load introduction, but also to identify implications on CFST column design and to develop suitable design guidance. Some of the advantages of CFST are the size of column is smaller, increases the usable floor area by 3.3% (5500m<sup>2</sup>), CFST columns used concrete 62% less and steel 5%~10% less than that of RC columns. Compared with steel column, CFST ones used steel is 50% less and decreases cost 45%. It is about 55% lighter than that of RC. Hence, the foundation cost can be reduced. The force resulting from earthquake is smaller. The cost on transportation and assembly of columns can be reduced because they are built by hoisting the empty steel tube first, then pour concrete into it. CFST columns are safer and more reliable in seismic region. The high-strength concrete can be used and the brittle failure can be prevented.

Many researchers agree that most composite structural elements are subjected to a multi-axial stress state. The response of concrete in CFST elements varies widely for different stress states, and it is therefore important to know how the concrete behaves in different multi-axial stress states. The structural behaviour of hollow CFST members is complex because of the interaction between the steel tubular shell and the hollow concrete core. The pioneer test research effort on the structural behaviour of CFST members was made by J. S. Sewel. He observed that the ultimate axial resistance of CFST columns is greater than the sum of resistance of separately tested steel and concrete components. Further investigations of CFST elements were performed by a great number of researchers of whom K. Klöppel and W. Guder, H. R. Salani and J. R. Sims, R. W. Furlong may be mentioned. Their investigations discovered that the increase in load-bearing capacity of CFST elements is mainly caused by the confining effect of steel tube on the concrete core. The different Poisson's ratios of steel tube and concrete core are considerably affected by the structural behaviour of CFST elements. Almost all researchers agreed that during the initial loading stage (as for solid as well as for hollow CFST members) the concrete Poisson's ratio is lower than that of steel (Fig 3a), and the steel tube has no confining effect on the concrete core. As longitudinal strains increase, the lateral expansion of concrete gradually becomes greater than that of steel tube (Fig 3b). Hoop and radial stresses are equal. At this stage, it is considered that the steel tube becomes bi-axially and solid concrete core triaxially stressed.

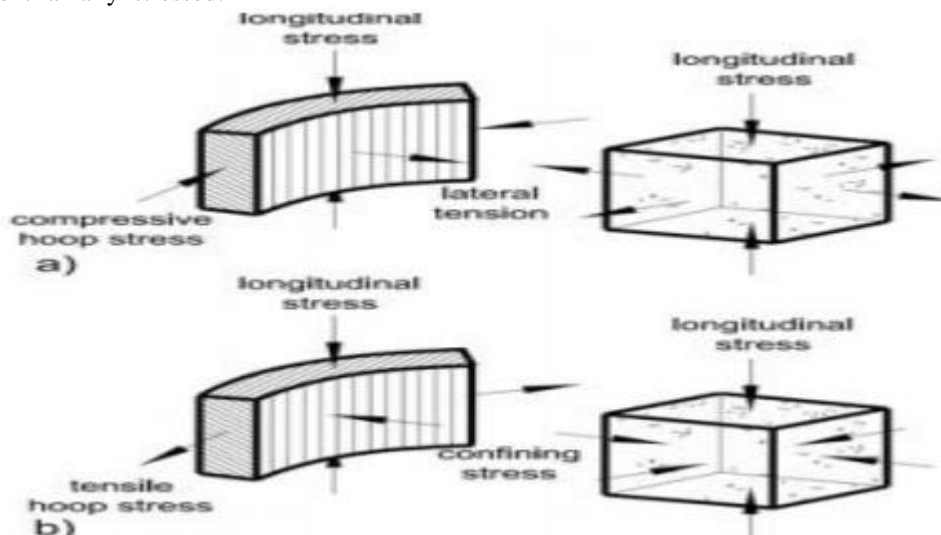


Fig.2 Stress condition in steel tube and concrete core at different stages of loading: (a)  $v_a > v_c$ , (b)  $v_a < v_c$

But for hollow CFST 3D stress state is on the inside concrete core and steel tube interface. At the same time, the steel is compressed in the longitudinal, radial and is tensioned in the hoop directions. For double-layered CFST (especially for layers from different concrete grades) the greater transversal deformations of internal layer cause lateral pressure on the external core layer. Thus stresses of both concrete layers redistribute, and on external concrete core layer maybe analysed as behaving in triaxial and internal, core layer - in biaxial states. On the other hand, researchers suggest for axially and laterally

compressed solid body to consider biaxial stress state as a simplified model of triaxial state.

But for hollow CFST 3D stress state is on the inside concrete core and steel tube interface. At the same time, the steel is compressed in the longitudinal, radial and is tensioned in the hoop directions. For double-layered CFST (especially for layers from different concrete grades) the greater transversal deformations of internal layer cause lateral pressure on the external core layer. Thus stresses of both concrete layers redistribute, and on external concrete core layer maybe analysed as behaving in triaxial and internal, core layer - inbiaxial states. On the other hand, researchers [12] suggest for axially and laterally compressed solid body to consider biaxial stress state as a simplified model of triaxial state.

In the first stage of axial compression the steel tube as a component of CFST element sustains a greater part of the load until it starts yielding. At this point a load transfer from steel tube to the concrete core starts, and a further increase of load is exhibited by only concrete core until it reaches its micro-cracking compressive strength. After this stage of loading, aredistribution of load from concrete core to the steel tube takes place. At this point the steel exhibits a hardening behaviour as in an uniaxial stress-strain hardening relationship.

The theoretical and practical investigations according to show that the behaviour of concrete in CFST elements becomes more ductile with lateral pressure increasing due to delaying micro-cracking. It is also interpreted that during compression the force transfer through concrete core is accomplished by bridging forces between the aggregates, and to a large extent by shear stresses, which are transferred over more or less inclined microcracks.

The lateral pressure force balances the bridging forces that reduce the tensile force and thereby delay the rise and growth of bond cracks, therefore formation of cracks becomes more difficult. According to above, when cracks are present, the confining stress will slow down shear sliding of cracks, due to an increase of the frictional shear stresses and stresses because of aggregate interlock. Furthermore, the reduced micro-cracking shear sliding leads to a less crack opening and thus reduces lateral expansion. A delayed damage due to confining pressure of maximum value is reached at zero volumetric strain of concrete. Another point of view to micro-cracking of concrete composite members is presented in this article. In composite steel and concrete structures, where one of main load bearing components is concrete, at various loading stages appear its compaction, resolution and failure processes, which lead to micro-cracking. During loading of concrete usually two parametrical points  $f_{cr0}$  and  $f_{crv}$  are fixed. Investigations allow defining consistent pattern relationships and various important concrete deformation processes between these points.  $f_{cr0}$  value of concrete strength notices the start of micro-cracking process and  $f_{crv}$  fixing the moment when of relative volume increment reaches zero. Independence of concrete structure parametric point  $f_{crv}$  is usually fixed when stresses in concrete core reach 0.5–0.8  $f_c$  value. Then concrete volume starts to increase, and at  $v_c \geq v_a$  a concrete core begins to stress a steel tube. For a certain period the micro-crack propagation process starts slowing down. However, further load increase leads to concrete core pressure rising on the steel shell. This phenomenon is considered as one of the main reasons of strengthening the concrete confined in the steel tube. At parametric point  $f_{crv}$  the increment of relative volume  $\Delta\theta$  reaches zero, and transversal strains of concrete core start to increase significantly. It is experimentally determined [16, 17] that structure of loaded concrete depends on the specimen form. Concrete tubes have a greater micro-cracking level  $v_{cr}$  or  $f_{cr}$  than prism or cylindrical specimens, because the values of transversal and longitudinal strains of concrete tubes are 1,2–1,3 times greater on internal than on external surfaces. For CFST elements under compression a parametrical point  $v_{cr}$  or  $f_{cr}$  maybe determined by condition  $\Delta\theta = 0$  [16]:

$$\Delta\theta = \frac{d_a^2(\Delta\epsilon_{lm} - 2\Delta\epsilon_{2e}) - d_i^2(\Delta\epsilon_{lm} - 2\Delta\epsilon_{2e})}{d_a^2 - d_i^2}, \quad (1)$$

where  $\Delta\epsilon_{lm} = \Delta\epsilon_e - \Delta\epsilon_{li}/2$  – mean increment of relative longitudinal strains at hollow CFST element on the external  $\Delta\epsilon_e$  and internal  $\Delta\epsilon_{li}$  surfaces, determined at corresponding loading step  $\Delta\sigma$ ;  $\Delta\epsilon_{2e}$ ,  $\Delta\epsilon_{2i}$  – transversal strains at external and internal surfaces of element respectively.

For the behavior in determining CFST members under axial compression the problem of axial symmetry is used. The behaviour of axial loaded centrifuged CFST members is more complicated than of a solid, because none of stresses are uniformly distributed through the cross-section, but the stress distribution pattern in the steel tube is the same both in solid and hollow composite cross-sections.

For 3D stress state the strain-stress relationship may be represented by generalised Hook's law, and the expression of longitudinal strains is derived from it:

$$\varepsilon_z = [\sigma_z - \nu(\sigma_r - \sigma_t)] / E \quad (2)$$

In plastic stage, the distribution of radial stress across hollow concrete core according to Lamé problem may be analysed as linear:

$$\sigma_r = \sigma_t (r_{ce} - r_{ci}) / (r_i - r_{bi}) \quad (3)$$

The distribution of hoop stress  $\sigma_t$  at plastic stage is due to rectangular diagram and its value defined by value of radial stresses due to Laplace equation:

$$\sigma_t = \sigma_r \beta i / (\beta i - 1) \quad (4)$$

where  $\beta i = r_{ce} / r_{ci}$  – relative concrete core thickness.

Behaviour of multi-layered hollow CFST elements is more complicated than of singlelayered ones because of additional interaction between concrete core layers (Figs 3 a,b, c). Eqs (2), (3) and (4) used for double- and triple-layered elements are valid only for the internal layer. As mentioned above, the 3D stress state is specific to external and media layers of hollow concrete core and stress determined as for solid member.

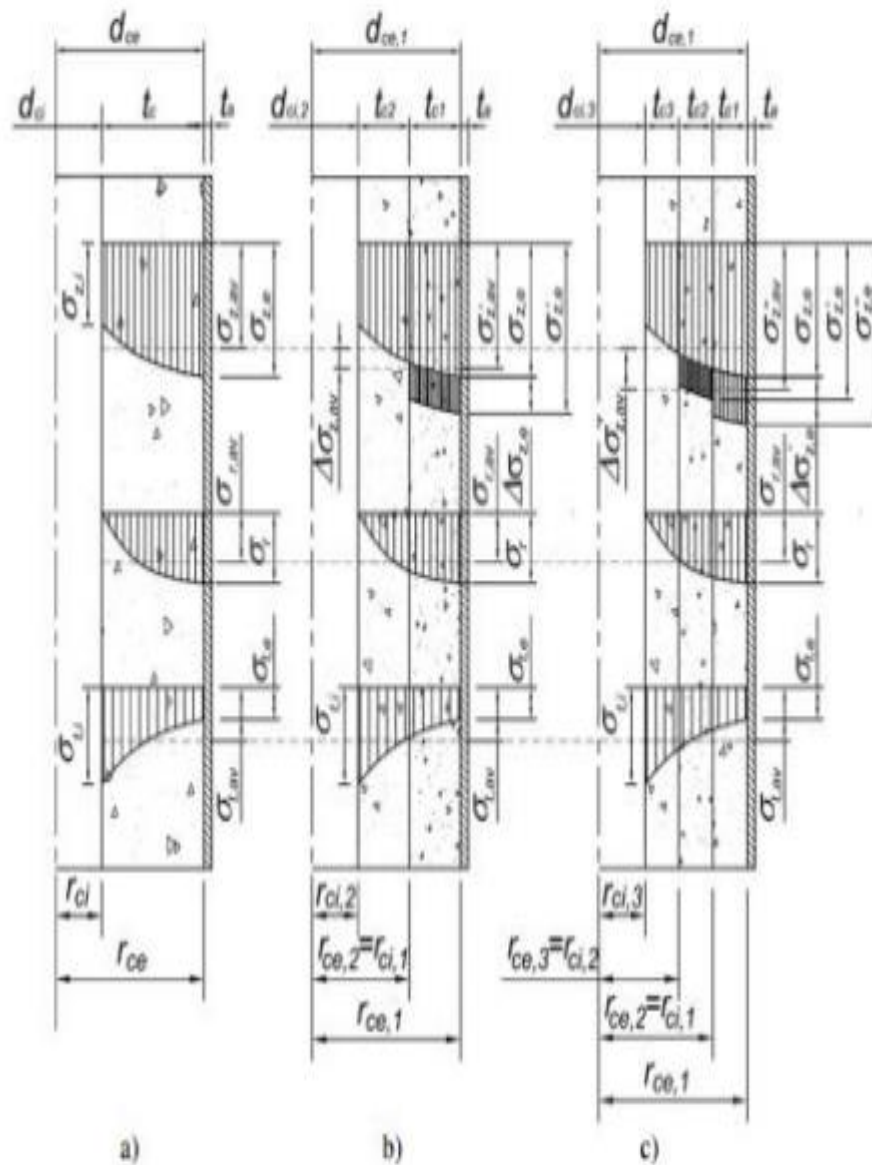


Fig 3. Stress distribution in concrete core of centrifuged (a), one- (b) double-, and (c) triple-layered CFST elements

## II. OBJECTIVES

Concrete filled circular tubular columns exhibit different patterns of cross-sectional stress distribution in concrete. In the case of circular columns, the cross-sectional stress distribution is uniform. The axial and lateral stress distributions at the cross section are radially uniform. Circular hollow sections provide a significant amount of confinement while this effect is negligible in the case of rectangular sections. Additional strength occurs because of the increase in compressive strength of the concrete core that is restrained laterally by the surrounding steel tube. This increase in concrete strength outweighs the reduction in the yield strength of steel in vertical compression due to the confinement tension needed to contain the concrete. Beyond this limit, steel exhibits a strain softening behaviour until it reaches the plastic limit. When the concrete reaches its maximum compression capacity, the steel tube exhibits a softening behaviour because a decrease in the stiffness of concrete core begins. The higher internal pressure causes larger hoop stress, which results in a reduction in compressive stress in steel tube. Short composite columns exhibit a failure mechanism characterized by yielding of steel and crushing of concrete. Medium length columns behave inelastically and fail by partial yielding of steel, crushing of concrete in compression and cracking of concrete in tension.

## III. METHODOLOGY

Steel circular hollow sections (CHS) were used in manufacturing the specimens. Yield and ultimate strength of CHS were determined by standard steel plate coupons and rings tests. The coupons and rings were cut off from each steel tube. According to test results the, S355 steel grade was found for CHS. The concrete mixture for single- and double-layered specimens was designed for compressive cube strength at 28 days of approx 30 MPa. The used mixture proportions are presented in Table 1. For fine aggregate the quartz sand of 0,2 mm main grain size and Portland cement of CEMII/A-L 42,5N grade as binder material were used. The initial cement/water ratio and slump of concrete cone were taken from recommendations, but because of very fine aggregates the required slump for centrifugation with these proportions of concrete components was not achieved. So for achieving the needed slump additional water was used (Table 1, number in brackets). After centrifuging the residual water quantity was measured, and it was obtained that during multi-layered centrifuging more residual water is pressed out from the concrete mixture. For determining the concrete, mechanical properties cubes and prisms were manufactured from the same concrete mix by vibrating. Single- and double-layered centrifuged CFST were cured in laboratory with environmental humidity of 21% and temperature 16,1 °C. Concrete cores in centrifuged specimens were isolated from environmental action by polyethylene film at the ends of steel tube. Internal environmental humidity was 82 %. CFST members after 28 days of curing were cut to smaller specimens of ~437 mm in length. For determining the mechanical properties of single- and double-layered centrifuged concrete cores the steel shells from some specimens were taken off. Hollow concrete and CFST elements were tested under an axial compression.

For the improvement that in hollow CFST elements during loading the stresses are redistributed in a complex way as mentioned above, there were manufactured and axially compressed specimens of annular cross-section: single- (1CFST) and double-layered (2CFST) CFST members (Fig c), single- (1CT) and double-layered (2CT) concrete members and empty steel tubes ST (Fig a). All their longitudinal  $\epsilon_L$  and transversal  $\epsilon_t$  strains measured by vertical and horizontal strain-gages, and load-bearing capacity were fixed by testing machine scale. These test results are presented in Table 2 and by  $F - \epsilon$ ,  $F - v$ ,  $v - \epsilon$  diagrams below.

The analysis of results shows that during multilayered centrifuging an interaction between components of CFST element appears and increases strength at least by 10 %. These results have shown that composite effect of single-layered specimens was ~6 %, for double-layered ~12 %. Diagrams  $F - \epsilon$  of ST members are presented in Fig 5a from which can be noted that yield stresses appear near the value determined by testing of rings  $340 f_{y,c} = \text{MPa}$  and coupons  $361 f_{y,t} = \text{MPa}$ . Buckling of ST members appears immediately after reaching the yield stresses.

Fig represents diagrams  $F - \epsilon$  of single- and double-layered CT. Curves 1, 1' in Figs b, c represent values of longitudinal and transversal strains measured on a single-layered internal, 3, 3' on external concrete core



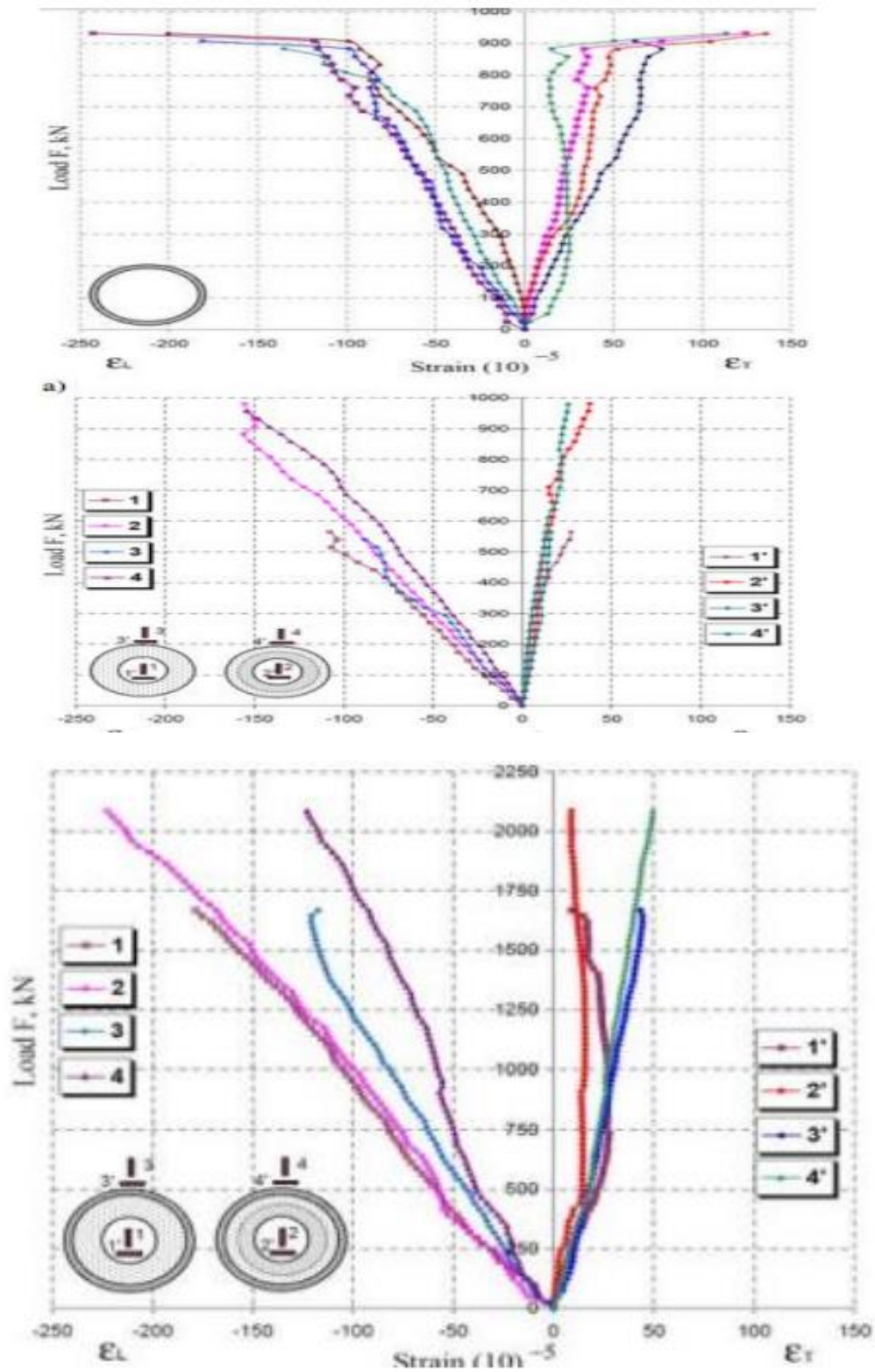


Fig 4 Diagrams  $F - \epsilon_i$  for ST (a); CT (b) and CFST (c) elements

Concrete confinement within a CFST column is well recognised (Chaudhari and Chakrabarti, 2012). In a CFST column, particularly when using a circular steel tube, the concrete is confined by the steel tube and is subjected to triaxial compressive stresses (Figure 5) (Hu et al., 2003). This happens as a result of the Poisson's ratio of the concrete core being greater than that of the steel when the concrete approaches failure.

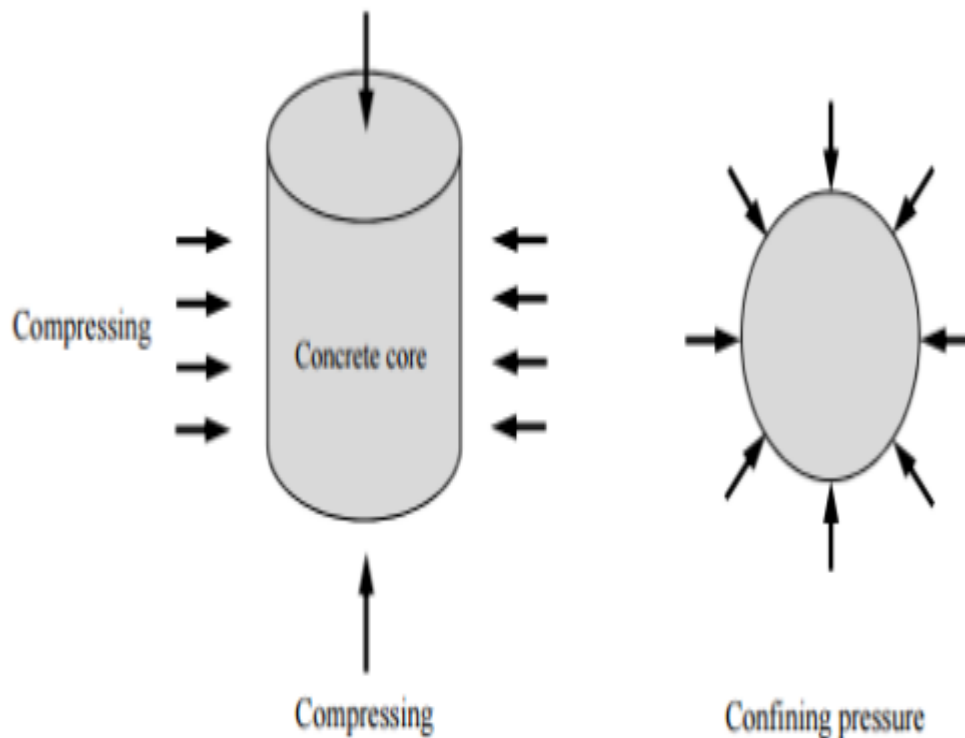


Fig.5 Concrete confined by the steel tube subjected to triaxial compressive stresses

The numerical model in this research will be established using the general finite element (FE) package ABAQUS. To simulate the concrete material in CFST columns, a linear Drucker-Prager yield criterion with associated flow rule model available in ABAQUS will be employed. The Drucker-Prager yield criterion is designed to model granular-like and frictional materials, such as soils and rock which exhibit pressure-dependent yield. It is also suitable for modelling materials which have considerably higher compressive yield strength than tensile yield strength (ABAQUS, 2012).

Concrete filled steel tubular columns are clearly an intermediate between steel and reinforced concrete columns. However, the design philosophy for each of these two structural members is fundamentally different. Steel columns are treated as concentric in that they are loaded through their centroids, but with due allowances being made for residual stresses, initial out of straightness and slight eccentricities of the load. The basis of the design of steel column is instability or buckling, and any moments which act at the ends of the column are then incorporated by reducing the axial load by way of an interaction equation. The approach for RC column is quite different from that for steel column in that the loads are considered to be eccentric to the centroid. The failure is generally, but not always, attributable to cross-sectional and material failure, and is based on the interaction curve as given in IS 456 -2000. Because of the similarity of CFST columns to both steel and concrete columns, there has been a great deal of debate by researchers as to which approach should be adopted. Short or stocky columns are clearly governed by cross section failure, while long or slender columns are prone to buckling. Perhaps the most logical treatment to date is that which is provided by the Eurocode 4. The behaviour of CFST columns can be best treated by a combination of both approaches.



#### IV. EXPERIMENTAL INVESTIGATION

Bond behaviour at the steel-concrete interface in a CFST column is mainly assessed by pushoff (Morishita et al., 1979a, Morishita et al., 1979b, Tomii et al., 1980a, Tomii et al., 1980b) and push-out tests (Roeder et al., 1999, Shakir-Khalil, 1993b, Parsley et al., 2000, Xu et al., 2009, Shakir-Khalil, 1991, Aly et al., 2010, Xiaowei and Xilin, 2010, Virdi and Dowling, 1975). Two types of boundary conditions are normally considered for push-out tests: (a) push-out test without shear tabs (Figure 2.7(a)); (b) push-out test with shear tabs (fin plate). These experimental configurations, however, do not share the same loading and boundary conditions as in a typical CFST column. Each of these tests has advantages and disadvantages in the assessment of the bond strength of CFSTs. The boundary conditions of push-out tests induce constant bond stress at the ultimate limit state and thus provide little information as to the distribution of bond stress along the length of the column. However, in push-off tests (Figure 2.7(b)), the bond stress is not constant and therefore it is difficult to accurately estimate the magnitude of the bond stress. In typical push-out and push-off tests, the specimen bears directly on a rigid support at the base excluding the beneficial effects that the shear connections provide.

However, in the push-out tests with shear tabs (Figure 2.7(c)), the force applied to the concrete core is resisted by the shear tabs attached to the steel tube which would be a reasonable representation of the realistic structures. In this condition, the bottom of the shear tabs rotates towards the CFST column and the top of the tabs rotates outwards thus inducing lateral stresses. Both cases develop considerable high contact pressure at the steel-concrete interface, which results in higher bond stresses there. Thus, these tests include the favourable effects that occur in typical beam-column connections due to the rotation of the shear tabs (Zhang et al., 2012).

- A. *Analysis* : Fig.3 shows the deformation behavior of circular and square CFST column under axial loading 3600KN. Fig. 4(a) illustrates the load versus deformation relationship of circular as well as square CFST member for grade of concrete 30 N/mm<sup>2</sup> under axial compression. Fig.4(b) shows the deformation of circular and square column for axial loading 3600KN for different grade of concrete (30, 50, 70, 90 N/mm<sup>2</sup>). It was found that, deformation in a circular CFST column is less than Deformation in Square CFST column. Less Deformation in circular section is due to higher moment of inertia and confining effect. Initially the load versus deformation behavior is linear, but later it attains ductility. Deformation decreases with increasing grade of concrete. For Axial load, deformation in circular section is 29.6, 19.5, 18.0, 16.3 percentage less than Square section for grade of concrete 30, 50, 70, 90 N/mm<sup>2</sup> respectively. Deformation decreases 18.2, 26, 31.5% with increasing grade of concrete from 30 N/mm<sup>2</sup> to 50, 70, 90 N/mm<sup>2</sup> respectively. For higher grade of concrete decreasing in deformation is less compared to normal strength of concrete.

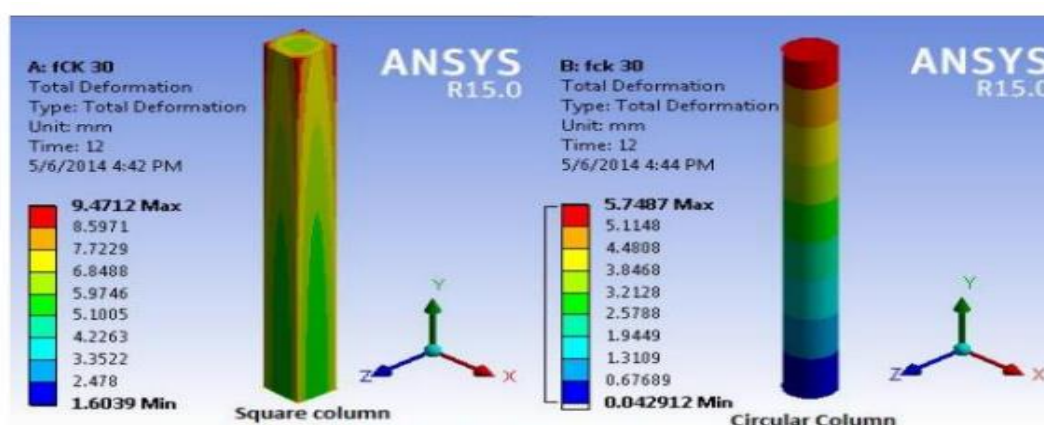


Fig 6 Deformation of Square and Circular Columns for Axial load of 3000 kN

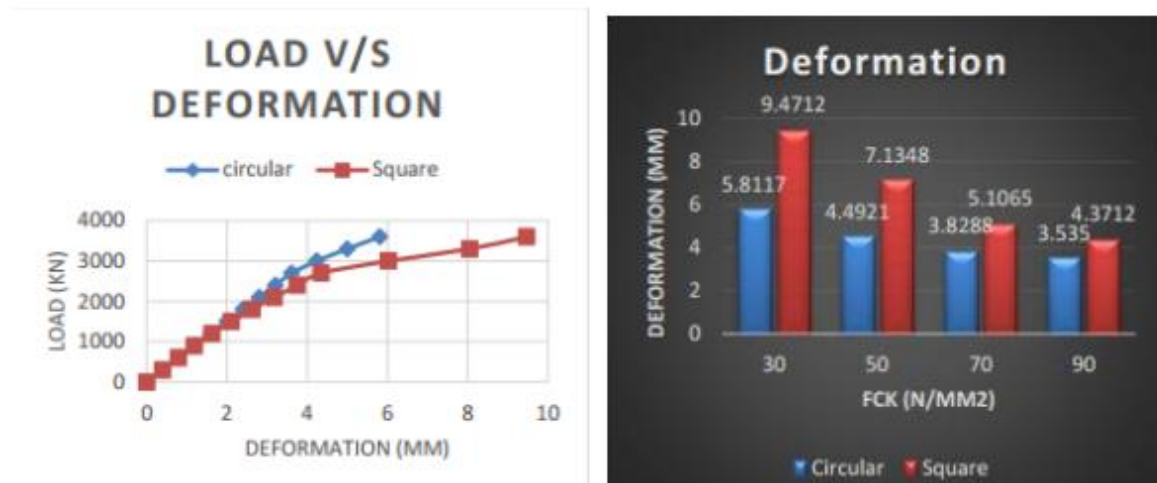


Fig.7 Load Versus Deformation Curve and Deformation for different grade of concrete

Percentage variation in deformation w.r.t. $f_{ck}$ 30 Mpa.		
Loading	Axial Load	
$F_{ck}$	Circular	Square
50	18.22	28.46
70	26.00	36.20
90	31.56	42.10

Table.I Percentage Variation of Deformation in circular and Square Columns w.r.t  $f_{ck} = 30$  Mpa

#### B. Procedure for Material Testing:

- Conduct an experimental testing program to study the performance of concrete filled steel tubes considering several parameters such as :
  - The compressive strength of the concrete infill.
  - The steel tube outer diameter to thickness ratio.
  - The loading rate.
  - The GFRP jacketing.
- Develop a finite element model using ABAQUS and verify it using the experimental results.
- Compare test results to theory and some codes formulae to illustrate their accuracy, such as:
  - Theoretical formulae.
  - American Institute of Steel Construction code formulae (AISC).
  - ACI 318 and AS codes formulae.
  - Giakoumelis G. and Lam D. formulae.
  - Mander et al. formulae.
  - Eurocode 4 formulae.

## V. RESULTS

### 1. Concrete Material Tests

#### 1.1 Cube Test :

Concrete cubes were cast from the same batches used to fill the CFST steel tubes. After 28 days of curing in water, ten standard size concrete cubes (150mm x 150mm x 150mm) were subjected to standard compressive test to determine the two concrete batches compressive

strengths, as shown in Table below.

$f'_c$	Sample Code	Mass of Specimen	Load	Stress	Avg. Mass (kg)	Avg. Peak Load (kN)	Avg. Max Stress (MPa)
		kg	kN	MPa			
High strength concrete cubes	cube-H1	8.3	4677	21	8.32	1568	70
	cube-H2	8.3	1571	70			
	cube-H3	8.3	1573	70			
	cube-H4	8.18	1536	68			
	cube-H5	8.5	1591	71			
Normal strength concrete cubes	cube-L1	8.45	1253	56	8.34	1197	53
	cube-L2	8.3	1179	52			
	cube-L3	8.3	1195	53			
	cube-L4	8.3	1073	48			
	cube-L5	8.34	1283	57			

As shown, the cubes are divided into two sets, one from high strength batch and the other is from the normal strength batch. It can be noted that the test results for specimen cube H1 varies from the others. This variation was a result of the stress concentration that took place while testing because of the unlevelled cube sides that was used by mistake.

Figure 14 shows the failure mode of one of the concrete cubes when tested after 28 days. The double coned failure was the dominant failure mode among all the cubes. This failure mode indicated a good distribution of particles and ingredients in the concrete mix. In addition, it shows an adequate bond between the cement paste and the aggregate. Also, it points out that the applied load is almost pure axial loading with minimal eccentricity if any.

## 1.2 Cylinder Test:

Just like the concrete cubes, the 12 concrete cylinders were cast from the same batch used to fill the CFST steel tubes, 6 from each batch. The concrete cylinders and the CFSTs were tested at the same time. The cylinders were subjected to high and normal loading rates similar to the ones applied to the CFSTs. The below table shows the summary of the results, where R60 and R0.6 refers to the loading rate of 60kN/s and 0.6kN/s, respectively. Also,  $f_{60}$  and  $f_{44}$  refers to the concrete's compressive strength of 60 MPa and 44 MPa,

ID	Ultimate Load	Ultimate Stress	AVG. Ultimate Load	AVG. Ultimate Stress
R <sub>60</sub> $f_{60}$ - 1	512	65	504	64
R <sub>60</sub> $f_{60}$ - 2	506	64		
R <sub>60</sub> $f_{60}$ - 3	493	63		
R <sub>60</sub> $f_{44}$ - 1	364	46	365	46
R <sub>60</sub> $f_{44}$ - 2	370	47		
R <sub>60</sub> $f_{44}$ - 3	359	46		
R <sub>0.6</sub> $f_{60}$ - 1	479	61	475	60
R <sub>0.6</sub> $f_{60}$ - 2	452	58		
R <sub>0.6</sub> $f_{60}$ - 3	493	63		
R <sub>0.6</sub> $f_{44}$ - 1	338	43	344	44
R <sub>0.6</sub> $f_{44}$ - 2	341	44		
R <sub>0.6</sub> $f_{44}$ - 3	352	45		

Ultimate load and stress carrying capacity of Cylindrical Sample The concrete cylinders subjected to high loading rate exhibited explosive failure regardless of their compressive strength. However, the specimens subjected to low rate of loading experienced shear failure unlike the concrete cube as shown in Figure 6.

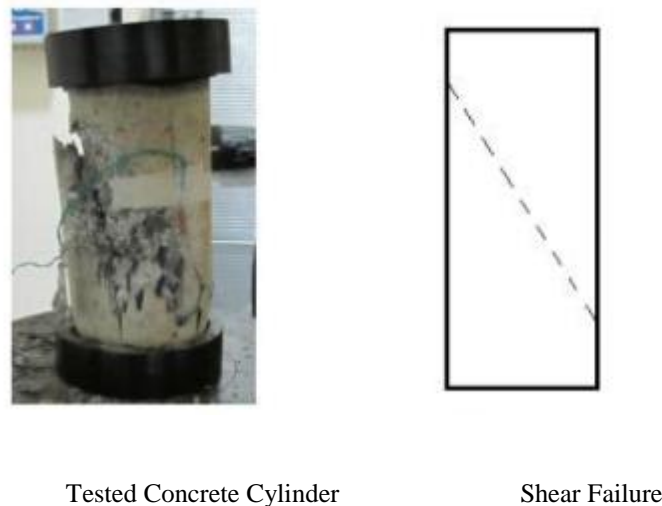
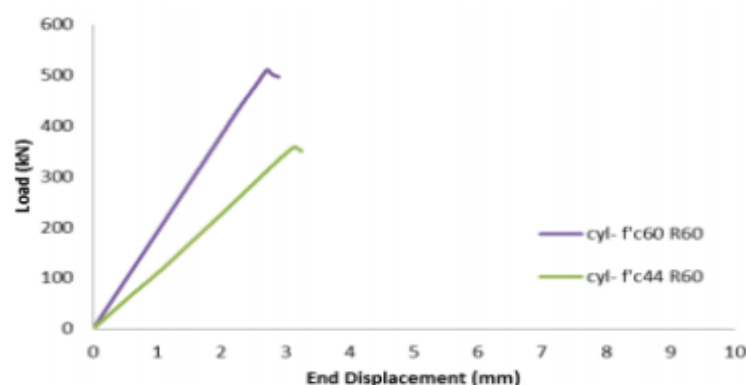


Fig.6 Low loading rate results in shear failure

Above figure shows the load-displacement diagrams of concrete cylinder with compressive strengths of 60MPa and 44MPa and subjected to loading rate of 60kN/s. Clearly, the stiffness of high compressive strength concrete is greater than the normal compressive strength concrete. It is noted that the absence of the nonlinear region in the two curves is due to the brittle nature of concrete in addition to the high loading rate.



## 2. Steel Material Tests:

### 2.1 Coupon Test:

Standard sized samples were prepared from each of the three steel tubes used to confine the concrete. The tested samples were loaded under three loading rates which are 2mm/min, 50mm/min, 500mm/min. using the measured dimensions of each sample and the data provided by the machine, the engineering stress and engineering strain values were calculated and presented in Table below.

Rate	ID	yield strain	yield stress (MPa)	Ultimate Strain	Ultimate Stress (MPa)	AVR. yield strain	AVR. yield stress (MPa)	AVR. Ultimate Strain	AVR. Ultimate Stress (MPa)
Normal rate 2 (mm/min)	t <sub>3.1</sub> R <sub>2</sub> -1	0.0124	352	0.2357	442	0.01329	352	0.2414	444
	t <sub>3.1</sub> R <sub>2</sub> -2	0.0142	351	0.2472	446				
	t <sub>5.6</sub> R <sub>2</sub> -1	0.0086	245	0.1454	316	0.00955	273	0.1430	332
	t <sub>5.6</sub> R <sub>2</sub> -2	0.0105	301	0.1405	349				
	t <sub>3.6</sub> R <sub>2</sub> -1	0.0139	335	0.2808	406	0.01370	350	0.2504	421
	t <sub>3.6</sub> R <sub>2</sub> -2	0.0135	365	0.2199	436				
Intermediate rate 50 (mm/min)	t <sub>3.1</sub> R <sub>50</sub> -1	0.0137	318	0.1515	456	0.01425	334	0.1415	456
	t <sub>3.1</sub> R <sub>50</sub> -2	0.0144	351	0.1261	460				
	t <sub>3.1</sub> R <sub>50</sub> -3	0.0147	331	0.1470	451				
	t <sub>5.6</sub> R <sub>50</sub> -1	0.0229	346	0.0818	409	0.02330	356	0.0765	416
	t <sub>5.6</sub> R <sub>50</sub> -2	0.0237	367	0.0712	424				
	t <sub>3.6</sub> R <sub>50</sub> -1	0.0145	337	0.1224	423	0.01551	339	0.1133	423
	t <sub>3.6</sub> R <sub>50</sub> -2	0.0165	340	0.1042	423				
High rate 500 (mm/min)	t <sub>3.1</sub> R <sub>500</sub> -1	0.0186	352	0.2547	462	0.02107	369	0.2483	466
	t <sub>3.1</sub> R <sub>500</sub> -2	0.0211	382	0.2399	471				
	t <sub>3.1</sub> R <sub>500</sub> -3	0.0235	373	0.2503	466				
	t <sub>5.6</sub> R <sub>500</sub> -1	0.0307	372	0.1935	422	0.03359	379	0.2070	430
	t <sub>5.6</sub> R <sub>500</sub> -2	0.0364	386	0.2205	437				
	t <sub>3.6</sub> R <sub>500</sub> -1	0.0251	373	0.2790	440	0.02472	370	0.2530	440
	t <sub>3.6</sub> R <sub>500</sub> -2	0.0243	367	0.2269	440				

Steel Coupon test results It should be noted that t<sub>3.1</sub>, t<sub>5.6</sub> and t<sub>3.6</sub> refer to the different steel tube thickness of 3.1mm, 3.6mm and 5.6mm, respectively. Similarly, R<sub>2</sub>, R<sub>50</sub> and R<sub>500</sub> refer to the different strain rates of 2mm/min, 50mm/min and 500mm/min, respectively. Since the properties of the steel samples are almost identical for the same strain rate, it is safe to assume that the material properties of the three steel tubes are similar. Note that the yield stress and the ultimate stress of the sample increase as the loading rate increases. It shows that one of the coupon samples tested under low strain rate. As expected, the failure of all samples took place in gage length segment of the specimen due to the reduction in the cross sectional area. In addition, all the samples displayed an acceptable amount of necking just before rupture as displayed in Figure 18. It should be mentioned that only one of the samples (t<sub>5.6</sub> R<sub>2</sub> -2) slipped from the machine grips during the test and it was done again. The slipping occurred because the grip areas of the specimens were manufactured based on the standard sizes, but the available grips of the testing machine were found to be slightly smaller.

## 2. Steel Tube Test:

A total of ten hollow steel tube specimens were loaded till failure. These samples were divided among the two loading rates, five for each. Table 16 shows the summary of the results where R<sub>60</sub> and R<sub>0.6</sub> refers to the loading rate of 60kN/s and 0.6kN/s, respectively. Also, t<sub>3.1</sub>, t<sub>5.6</sub> and t<sub>3.6</sub> refer to the steel tube thickness of 3.1mm, 3.6mm, and 5.6mm, respectively.

ID	Ultimate Load	Ultimate Stress	AVR. Ultimate Load	AVR. Ultimate Stress
tube t <sub>3,1</sub> R <sub>60</sub> -1	563	677	-	-
tube t <sub>5,6</sub> R <sub>60</sub> -1	789	807	789	807
tube t <sub>5,6</sub> R <sub>60</sub> -2	789	807		
tube t <sub>3,6</sub> R <sub>60</sub> -1	480	757	481	758
tube t <sub>3,6</sub> R <sub>60</sub> -2	482	759		
tube t <sub>3,1</sub> R <sub>0,6</sub> -1	556	668	-	-
tube t <sub>5,6</sub> R <sub>0,6</sub> -1	766	784	767	784
tube t <sub>5,6</sub> R <sub>0,6</sub> -2	767	784		
tube t <sub>3,6</sub> R <sub>0,6</sub> -1	464	731	467	736
tube t <sub>3,6</sub> R <sub>0,6</sub> -2	471	742		

Empty steel tubes test results Figure shows the stress-displacement diagrams of hollow steel tubes with a thickness of 5.6mm and an outer diameter of 114mm. the graph shows the effect of different loading rates R60 and R0.6 which corresponds to 60kN/s and 0.6kN/s, respectively. Apparently, the stiffness of the empty steel tubes is not affected by the change in the loading rate. On the other hand, the yield and the ultimate stresses have marginally increased with the increase of the loading rate due to the effects of the high loading rates on the behavior of the material as illustrated in the introduction chapter. In addition, the ductility of this section is not influenced by the loading rate.

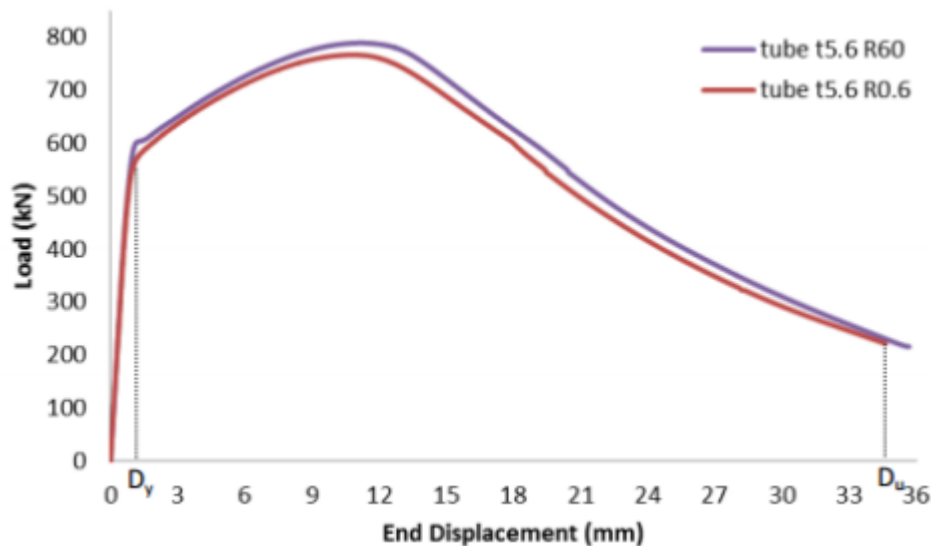


Fig. Stress- End Displacement diagram of empty steel tubes under various loading conditions

#### 4. Behaviour During Loading

##### 4.1 Stage one

In the initial concentric axial loading stages of the CFST column, both concrete infill and structural steel will deform longitudinally. Of course, it is assumed that the concentric loading is applied uniformly across the CFST section. The Poisson's ratio of the concrete infill (ranges between 0.15-0.25) is



smaller than that of structural steel (roughly 0.28) at these initial strains. Thus, the lateral expansion of the confining tube is larger than the confined concrete. As a result, localized separation between the two composite materials takes place along the column. Moreover, minimal interaction between the two materials occurs if any. The concrete and the steel bear their shares of the applied load independently during this phase. At a certain strain, the expansion of the concrete infill laterally increases until it reaches the lateral expansion of the steel. Keep in mind that the structural steel expansion remains constant in this stage and micro-cracking in the concrete begins to take place. This acceleration in the concrete expansion results in an interactive contact between the two materials. Hence, bond stresses are developed and the concrete will be subjected to tri-axial stresses while the structural steel to biaxial stresses [3]. Longitudinal stress in the confining tube varies based on the transfer of force between the concrete and steel. The strain level at which confinement occurs is debated among researchers to range from 0.001 to 0.002. Some scientists such as Knowles and Park concluded that concrete confinement happens suddenly at about (strain of 0.002) just as the concrete starts dilation. While other researchers as Tsuji, et al. and Zhang, et al. proposed a steady increase in the concrete confinement starting right after the occurrence of micro-cracking in the concrete (strain of 0.001), till full confinement is met at a strain around 0.002.

#### 4.2 Stage Two:

In the second stage of loading where the confinement of the steel tube on the concrete is present, circumferential stresses are developed in the structural steel due to two factors:

1. Longitudinal stresses from loading
2. Lateral pressure from concrete dilation.

Based on the steel utilized in the composite element, the steel could have reached its capacity prior to their yield in this stage. If tube yielding occurs before this biaxial state of stress, the tube would not be able to sustain the normal yield stress, resulting in a transfer of load from tube to the concrete core. Conversely, if the confining tube has not yet yielded, the extra axial capacity needed from the steel tube before yielding will be reduced [7]. Unlike the effective biaxial state of stress on the steel tube capacity, the concrete infill performance enhances when experiencing triaxial state of stress. The presence of confinement on the concrete infill increases its axial capacity. Despite the decrease in its steel tube capacity, the circular CFST column's overall capacity increases because the increase in the concrete infill capacity due to confinement is far greater than the strength loss in the steel tube.

## VI. CONCLUSION AND APPLICATIONS

### 1. Introduction

Most design engineers have treated the CFST system as an alternative to the steel system, trying to cut the cost by reducing the steel consumption. However, it is also possible to look at the CFST system as an alternative to the reinforced concrete system. In this study, three dimensional finite element models have been developed to investigate the force transfer by natural bond and the interaction between the steel tube and the concrete core of concrete-filled steel tubes under loading. Both material and geometric nonlinearities are considered in the analysis. Concrete filled steel tubular columns axial capacity significantly affected by the cross-section of the column, concrete's compressive strength and yield strength of the steel tubes.

### 2. Conclusion

Theoretical and experimental investigations show that behaviour of hollow CFST elements is more complicated than that of solid ones, because of complex stress states none of stresses in hollow concrete core are evenly distributed through the thickness of its cross-sections. For single-layered CFST elements the triaxial stress state is achieved only at the contact surface between the concrete core and steel shell. An internal hollow concrete core of double-layered CFST elements is in the same stress state as of single-layered members, but an external layer is analysed as being in 3D stress state. Researchers using materials of different properties tried to explain and evaluate this phenomenon by mathematical equations as stated above. During loading between neighbouring layers of concrete core in normal stress diagrams at place of interaction surface the step appears, and authors suggest how to evaluate this step. Test results improve the propositions of that multi-layered elements had greater load-bearing capacity with respect to single-layered hollow CFST elements. This increase in strength is explained by appearance of

additional interaction between neighbouring concrete layers under loading conditions. For double-layered CFST members greater deformations of an internal layer cause confinement of an external layer; therefore their stresses redistribute and an external concrete layer may be analysed as in 3D stress state. Behaviour of single- and multi-layered CFST elements differs essentially. Multi-layered elements resist not only greater loads but, being more ductile, they have better such characteristics as modulus of elasticity, density etc. Failure of such elements is more ductile, therefore structures from such elements may be used more safely. Experimental investigations presented in this article may help for further investigations and design of hollow single- and multi-layered CFST elements. Prediction of their behaviour at various loading situations is possible.

### 3. Need For Future Work

Concrete filled steel tubular (CFST) arch bridges have been building in China since 1990 under the background of fast development of economy and the requirements of sound highway networks. CFST members have better strength than those of masonry or reinforced concrete and can provide larger stiffness than steel tubes. An interactive force under axial compression confines the concrete core, which greatly improves its load-carrying capacity and ductility, and also delays the steel tube from local buckling. As a result, the spans of arch bridges can be enlarged with the use of CFST members. Another important advantage of the CFST arch bridges is that the thin-walled steel tubular arch itself can be erected with lower self-weight than concrete members and more outstanding stiffness than shaped steel members. The erected steel tubular arch can be filled with concrete without falsework and formwork. This makes the erection of arch bridges with long spans possible, improves the construction speed and saves the cost for construction. The structural configuration of CFST arch bridges can be divided into many types. The arch rib may consist of a singular tube or dumbbell section with two tubes or a trussed form with more than two tubes. Depending on the deck location in vertical direction, there are deck arch, through arch and half-through arch bridges. Both through arch and half-through arch configuration are most widely used in CFST arch bridge in China. The CFST arch bridges can also be classified into lateral bracing, no bracing, lift-basket arch bridges according to lateral connection. Additionally, according to thrust in an arch to the substructure, there are true arch bridge and tied arch bridge.

## REFERENCES

- [1] F.R Mashiri and A Paradowska, "Measurement of stress in steel tubes using neutron diffraction method" 5th international conference on advance in experimental structural engineering, nov 8-9, 2013, Taipei, Taiwan.
- [2] Suliman Hassan Abdulla, "Behaviour of concrete filled steel tube under different loading", A Thesis Presented to the Faculty of the American University of Sharjah, 2009
- [3] Tiziano Perea, "Behaviour of composite CFT beam – columns based on nonlinear fiber element analysis", Georgia Institute of Technology 2009.
- [4] T. Perea and R.T. Leon, "Composite cfst columns performance based on nonlinear analysis", The 14 World Conference on Earthquake Engineering October 12-17, 2008, Beijing, China.
- [5] Uwe Starossek, Nabil Falah and Thomas Lohning, "Numerical Analyses of the Force Transfer in Concrete-Filled Steel Tube Columns," 4th International Conference on Advances in Structural Engineering and Mechanics (ASEM'08) Jeju, Korea, May 26 -28, 2008.
- [6] Aaron w Malone, "Concrete filled steel tubular columns, a finite element study", Dept of civil engineering 2008, Marston Hall Amherst.
- [7] Artiomas kuranovas, Audronis Kazimieras Kvedaras, "Behaviour of hollow concrete filled steel tubular", Journal of civil engineering and management 2007, vol XIII, no 2, 131-14.
- [8] Furlong RW. Strength of steel-encased concrete beam-columns. J Struct Eng ASCE 1997;93(5):113-24.
- [9] Knowles RB, Park R. Strength of concrete-filled steel tubular columns. J Struct Div ASCE 1969;95(12):2565-87.
- [10] Schneider SP. Axially loaded concrete-filled steel tubes. J Struct Eng ASCE 1998;124(10):1125-38.
- [11] Sakino K, Nakahara H, Morino S, Nishiyama I. Behavior of centrally loaded concrete-filled steel-tube short columns. J Struct Eng ASCE 2004;130(2):180-8.
- [12] Fujimoto T, Mukai A, Nishiyama I, Sakino K. J Struct Eng Behavior of eccentrically 74) 461-80.